Chapter 5
The Speed of Spatial Spread

Abstract When a population can persist in a certain environment, we expect that it will spread through that environment if it is initially spatially confined to some small region. How fast will this spatial spread occur? How does the speed depend on movement behavior? These questions are particularly relevant for understanding and managing biological invasions. Spreading nonnative species can cause great damage to existing local ecosystems, e.g., by replacing native species or introducing pathogens. We need insights that help us decide between different management options to slow or contain the spread of harmful species. IDEs are particularly well suited to addressing the question of how different dispersal patterns influence the speed of spread. We begin this chapter with two different scenarios for spatial spread and explicit calculations for the linear growth function. We denote these as the *point-release scenario* and the *traveling-front scenario*. Then we define the *asymptotic spreading speed* and present the results for the nonlinear theory. Throughout the chapter, we assume that there is no Allee effect; we will devote Chap. 6 to it.

5.1 Measuring Spread

Before we can investigate how fast a locally introduced population spreads, we need to find a way to measure the rate of spread. It would be natural to try to find the speed of the "edge" of the population distribution, where the density transitions from positive to zero. However, we will see in our model that the population density is typically positive everywhere from the first generation on, even if the initial density has compact support. This phenomenon of "infinite spread" also occurs in reaction–diffusion equations, thus has long been studied and criticized (Einstein 1906). It is also not clear whether we can expect such a sharp edge to exist in real biological invasions. Individuals can be extremely difficult to detect at low population densities, so that a sharp edge, even if it existed, may be impossible to find. Instead, we consider two measures: in the *point-release scenario*, we track a threshold density; in the *traveling-front scenario*, we track an entire solution profile. A third measure, the *asymptotic spreading speed*, will be mathematically

© Springer Nature Switzerland AG 2019

F. Lutscher, *Integrodifference Equations in Spatial Ecology*, Interdisciplinary Applied Mathematics 49, https://doi.org/10.1007/978-3-030-29294-2_5

most satisfying, connecting the two former measures, but also analytically most challenging to handle.

Much of the content of this chapter can be traced back to two landmark papers: Weinberger (1982) proves the existence of an asymptotic spreading speed and traveling waves for a large class of operators that includes the integral operator in (5.1) below. Kot et al. (1996) highlight the value of IDEs to invasion biology by describing the effect of different dispersal kernels on invasion speed and finding accelerating invasions. Kot (2003) gives a first review of spread phenomena in IDEs and relates the findings to various biological invasions. The recent book by Lewis et al. (2016) provides an excellent introduction to many mathematical theories (including IDEs) of biological invasions.

To consider questions of spatial spread, we envision a scenario where the potential habitat of a population is so large compared to its actual spatial extent that an increase in the extent is not limited by the availability of habitat. Therefore, we consider the potential habitat to be the entire real line. For simplicity, we also assume that the habitat is homogeneous and that dispersal is unbiased. Then the dispersal kernel is a function of distance only, i.e., $K(x, y) = \widetilde{K}(x - y)$, where $\widetilde{K}$ is an even function. For notational simplicity, we drop the tilde. Hence, the IDE reads

$$N_{t+1}(x) = Q[N_t](x) = \int_{-\infty}^{\infty} K(x - y)F(N_t(y))\mathrm{d}y\,. \tag{5.1}$$

To ease notation, we frequently denote the convolution integral as $K * F(N_t)$. In this chapter, we shall assume that there is no Allee effect so that $F(N) \leq F'(0)N$. As we did for the question of population persistence, we begin our investigation of spreading phenomena with the linear model

$$N_{t+1}(x) = R\int_{-\infty}^{\infty} K(x - y)N_t(y)\mathrm{d}y = R(K * N_t)(x)\,, \tag{5.2}$$

where many of the relevant quantities and interesting phenomena can be calculated explicitly in special cases.

5.2 Spread from Point Release

Some biological invasions are initiated by a small number of individuals released at a single location outside their native habitat. For example, house finches (*Carpodacus mexicanus*) were illegally released in New York in the 1950s and spread westward (Veit and Lewis 1996). Shipping points for international trade are particularly prominent spots for invasions to emerge. The emerald ash borer (*Agrilus planipennis Fairmaire*) was transported in shipping and packaging material to the Detroit area from Asia and started spreading to many states and Canadian provinces from there in the late 1990s (Cappaert et al. 2005).

Mathematically, we idealize this point release of individuals by choosing a Dirac delta distribution $N_0(x) = \delta(x)$ as the initial condition. Recall that $\delta(x)$ can formally be thought of as a limit of top-hat functions (Table 3.1) when $\beta \to 0$ and the integral is constant. The delta distribution behaves particularly nicely under convolutions in that $f(x) = (f * \delta)(x)$ for all continuous functions f. More details on distributions and their properties can be found in many textbooks, e.g., Keener (2000).

Using the convolution property, we can calculate the solution of (5.2) with this initial condition explicitly as

$$N_t(x) = R^t K^{*t}(x)\,, \tag{5.3}$$

where K^{*t} denotes the t-fold convolution integral.

While formula (5.3) is elegant in its simplicity, its usefulness is somewhat limited because we can calculate this t-fold convolution only for a few dispersal kernels. We give two examples that show markedly different behavior.

Point Release and the Gaussian Kernel

The t-fold convolution of a Gaussian kernel with mean zero and variance σ^2 is a Gaussian kernel with mean zero and variance $t\sigma^2$. Therefore, if K is a Gaussian kernel with variance σ^2, then (5.3) becomes

$$N_t(x) = \frac{R^t}{\sqrt{2t\sigma^2\pi}} \mathrm{e}^{-\frac{x^2}{2t\sigma^2}}\,, \tag{5.4}$$

as illustrated in Fig. 5.1. We observe that even if the initial population is concentrated at a single point, the population density in the first (and every subsequent) generation is positive everywhere. This example illustrates the phenomenon of infinitely fast propagation. As discussed above, we cannot simply define a speed of propagation by tracking the spatial location where the population density becomes positive.

A *detection threshold* is a minimal density above which one has a reasonable and consistent chance to detect the presence of a particular species in empirical work. For example, the emerald ash borer lays eggs under the bark high up in trees. The exit holes of larvae are very small. The only way to detect a small density is to fell and debark every tree in question. While this can and has been done under special circumstances on a small scale (Mercader et al. 2009), it is not feasible and is obviously harmful on large scales. At higher density, the eggs will be placed lower in the tree, and the many exit holes will be easier to spot.

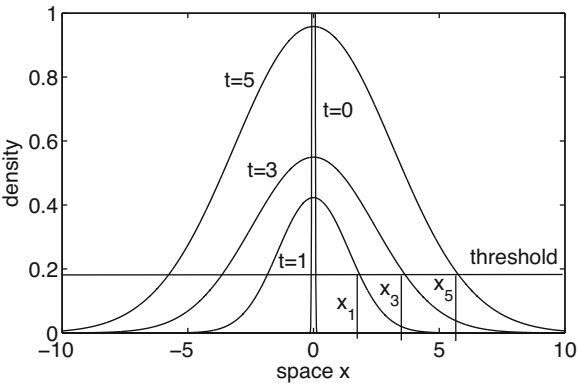

Fig. 5.1 Population spread from a point release at $x = 0$ with Gaussian dispersal kernel according to (5.3). The intersection with the detection threshold (horizontal line) defines the points x_t (see text). Parameters are $\sigma^2 = 2$ and $R = 1.5$.

In mathematical terms, we define $\widetilde{N}$ as the detection threshold, and we set x_t as the rightmost location at which the population exceeds this threshold in generation t; see Fig. 5.1. The defining equation for x_t,

$$\widetilde{N} = \frac{R^t}{\sqrt{2t\sigma^2\pi}} \mathrm{e}^{-\frac{x_t^2}{2t\sigma^2}} , \tag{5.5}$$

can be solved (provided $\widetilde{N}$ is small enough) to get

$$x_t = \sqrt{2t^2\sigma^2 \ln R - 2t\sigma^2 \ln\left(\sqrt{2t\sigma^2\pi}\,\widetilde{N}\right)} . \tag{5.6}$$

To calculate a speed, we recall that the population was initially located at $x = 0$, so that the distance covered per unit time is given by x_t/t. This number depends on the detection threshold and changes over time, but in the limit, we obtain a speed that depends only on the two model parameters:

$$\lim_{t\to\infty} \frac{x_t}{t} = \sqrt{2\sigma^2 \ln(R)} =: c_G . \tag{5.7}$$

Hence, asymptotically, the population spreads in space with constant speed (displacement per generation). In general, this speed is denoted by c; the subscript G indicates that the expression in (5.7) is obtained specifically with the Gaussian kernel.

Point Release and the Cauchy Kernel

The *Cauchy kernel* is defined as

$$K(x) = \frac{1}{\pi} \frac{\beta}{\beta^2 + x^2} . \tag{5.8}$$

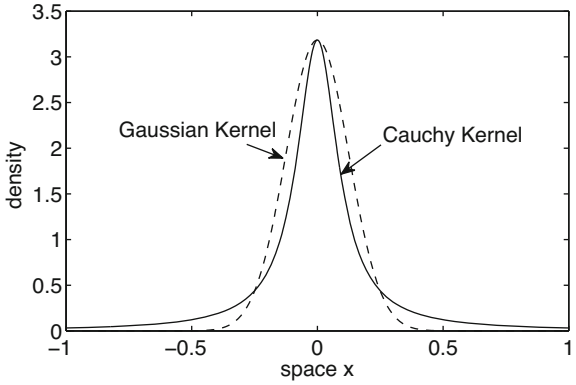

Fig. 5.2 The Gaussian (dashed) and the Cauchy (solid) dispersal kernel. We set $\beta = 0.1$ and choose $\sigma^2 = \pi\beta/2$ such that the two kernels agree at $x = 0$.

It describes a fat-tailed distribution, where dispersal distances follow a power law decay. Hence, they decay much more slowly than for the Gaussian or the Laplace kernel (Fig. 5.2). This kernel has no well-defined variance. In fact, all the moments of this distribution are infinite. Nonetheless, we can calculate the t-fold convolution for this kernel via Fourier transforms.

Following Kot et al. (1996), we use the (scaled) Fourier transform

$$\widehat{N}(\omega) = \int_{-\infty}^{\infty} N(x) \mathrm{e}^{\mathrm{i}\omega x} \mathrm{d}x \,. \tag{5.9}$$

The Fourier transform is particularly well suited for this situation since it turns convolutions into multiplications via a change of variables:

$$\begin{aligned} \widehat{K * K}(\omega) &= \int_{-\infty}^{\infty} \int_{-\infty}^{\infty} K(x-y) K(y) \mathrm{e}^{\mathrm{i}\omega x} \mathrm{d}y \mathrm{d}x \\ &= \int_{-\infty}^{\infty} K(y) \mathrm{e}^{\mathrm{i}\omega y} \mathrm{d}y \int_{-\infty}^{\infty} K(z) \mathrm{e}^{\mathrm{i}\omega z} \mathrm{d}z = \widehat{K}(\omega) \cdot \widehat{K}(\omega) \,. \end{aligned} \tag{5.10}$$

Hence, the t-fold convolution in (5.3) becomes the product $\widehat{N}_t(\omega) = R^t \widehat{K}^t(\omega)$. So far, the calculations are general. The challenge now is to find the inverse Fourier transform of this expression. Numerically, this can be done using the fast Fourier transform (FFT) and its inverse. This procedure will be the basis for one numerical method of solving IDEs (Chap. 8). For the Cauchy kernel, the inverse can be found analytically.

The Fourier transform of the Cauchy kernel in (5.8) is

$$\widehat{K}(\omega) = \mathrm{e}^{-\beta|\omega|} \,. \tag{5.11}$$

Its t-fold product, $\widehat{K}^t(\omega) = \exp(-\beta t|\omega|)$, is of the same form, so that the inverse transform of $\widehat{N}_t(\omega) = R^t \widehat{K}^t(\omega)$ must be

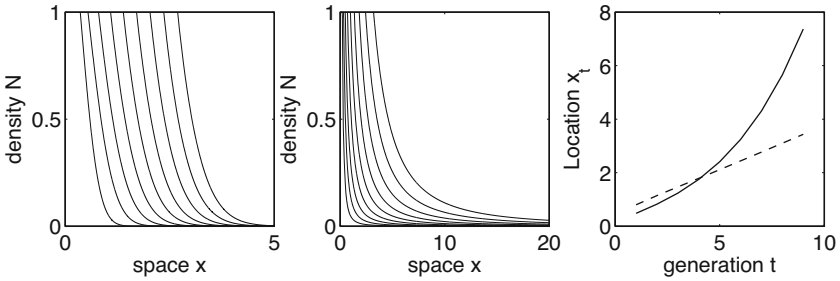

Fig. 5.3 Population spread from a point release at $x = 0$. **Left plot:** Spread with Gaussian kernel (2.25). **Middle plot:** Spread with Cauchy kernel (5.8). **Right plot:** Location x_t of the level set $N_t(x_t) = 0.2$. Parameters are $\beta = 0.1$, $\sigma^2 = \pi\beta/2$, and $R = 1.5$. Population densities are plotted for 10 generations. We note the difference in scale on the x-axis.

$$N_t(x) = \frac{R^t}{\pi} \frac{\beta t}{\beta^2 t^2 + x^2} \,. \tag{5.12}$$

The rightmost location where the population exceeds threshold $\widetilde{N}$ is given by

$$x_t = \sqrt{\frac{R^t \beta t}{\widetilde{N}\pi} - \beta^2 t^2} \,. \tag{5.13}$$

This expression grows faster than geometrically in time. In particular, there is no asymptotically constant speed of spread. The distance that the population moves per generation increases faster than linearly with each generation, so that $\lim_{t\to\infty} x_t/t = \infty$. A comparison between this behavior and the asymptotically constant speed is illustrated in Fig. 5.3. We call this phenomenon an *accelerating invasion*. As an ecological consequence, a biological invasion could speed up over time, and its location would be much harder, if not impossible, to predict.

The difference between propagation according to the Gaussian kernel with asymptotically constant speed and the Cauchy kernel with continuously accelerating speed is striking. Which properties of a dispersal kernel ensure that propagation occurs at an asymptotically constant speed? In the next section, we present a second approach to defining and calculating a measure for spatial spread. This approach will lead us to the criterion we seek.

5.3 Spread as Traveling Fronts

The preceding calculations for x_t require an explicit solution of the IDE, but that is generally not available. The right plot in Fig. 5.3 suggests the existence of solutions

in the form of a *traveling front*,[1] i.e., a fixed spatial profile that is shifted by a fixed distance per generation. If we *assume* that such fronts exist, we can derive conditions on their speed from the model parameters. A traveling front describes the density of a species that is well established over a large area and continues to expand its range. This situation might occur long after an initial point release (see above) or could arise as conditions at the range boundary change, e.g., when global change opens climatic opportunities for species to expand their ranges poleward.

We denote by $N^*(x)$ the profile of the front in some generation and by c the displacement per generation. Then the profile in the next generation is $N^*(x-c)$. We substitute this expression into the linear equation (5.2) and obtain the relation

$$N^*(x-c) = R\int_{-\infty}^{\infty} K(x-y)N^*(y)\mathrm{d}y\,. \tag{5.14}$$

Since the equation is linear, we make the exponential ansatz $N^*(x) = \exp(-sx)$. To mimic the simulations in Fig. 5.3, we consider a rightward-moving ($c > 0$), monotone-decreasing ($s > 0$) profile. Substituting the exponential ansatz into (5.14), we obtain the relationship

$$\mathrm{e}^{sc} = R\int_{-\infty}^{\infty} K(y)\mathrm{e}^{sy}\mathrm{d}y =: RM(s)\,. \tag{5.15}$$

Function M, defined in (5.15), is called the *moment-generating function* of the kernel. By definition, it satisfies $M(0) = 1$. For $s \neq 0$, the value $M(s)$ is finite only if the tails of the kernel decay to zero faster than $\exp(-sx)$. If $M(s)$ is finite for at least one nonzero value of s, we say that the kernel is *exponentially bounded*. The Gaussian kernel is exponentially bounded, but the Cauchy kernel is not. This difference will explain the different spreading behavior that we found in the previous section.

There is an alternative way to derive relation (5.15) by a so-called exponential transform: One multiplies both sides of (5.14) by e^{sx} and integrates with respect to x. This latter approach has the advantage that it does not assume a particular shape of the profile $N^*(x)$, only that it be exponentially bounded. The former approach, on the other hand, allows us to interpret parameter s as the steepness of the invasion front.

[1] A note on terminology is in order. The terms *traveling front*, *traveling wave*, and *traveling profile* may mean the same or slightly different things to different authors. Some authors use *constant-speed traveling front* to be more specific. Some authors require that a traveling front be bounded, while others require monotonicity in addition. In the linear equation that we study in this section, one cannot expect nontrivial bounded traveling fronts. We will use the terms interchangeably and qualify additional properties if necessary.

We can solve (5.15) for c and obtain the *dispersion relation*

$$c = c(s) = \frac{1}{s} \ln(RM(s)), \qquad s > 0, \tag{5.16}$$

that determines the speed at which an exponential profile with parameter s travels. Since $M(0) = 1$, we have $c(s) \to \infty$ as $s \to 0$. Consequently, a flat front will travel fast. Typically, the moment-generating function increases at least exponentially in s while it exists, so that $c(s)$ is large for large values of s as well. (We give a few examples later when we discuss approximations to the spreading speed for several kernels; see Table 10.1.) Consequently, a steep front will travel fast. One can show that $c(s)$ cannot have a local maximum, so that a minimum, if it exists, must be unique.

Lemma 5.1 *Assume that K is symmetric and that the moment-generating function M of K is defined for some positive value of s. Then the function $c = c(s)$ from (5.16) is defined on some (possibly unbounded) interval. Furthermore, c has no local maximum and at most one local minimum, which—if it exists—is the global minimum.*

Proof The proof follows Weinberger (1978); see also Bourgeois (2016). Since the kernel is nonnegative and symmetric, the moment-generating function is increasing in $s > 0$. Hence, if $M(s)$ is finite for some $s > 0$, then it is finite for the entire interval $[0, s]$.

We define the function

$$\Psi(s) = \frac{\int x \mathrm{e}^{sx} K(x) \mathrm{d}x}{\int \mathrm{e}^{sx} K(x) \mathrm{d}x} .$$

By differentiation, we find

$$c'(s) = -\frac{1}{s}[c(s) - \Psi(s)] \quad \text{and} \quad c''(s) = \frac{1}{s^2}[c(s) - \Psi(s)] - \frac{1}{s}[c'(s) - \Psi'(s)] .$$

Substituting and multiplying by s^2, we find $(s^2 c'(s))' = s\Psi'(s)$. We calculate

$$\Psi'(s) = \frac{\int [x - \Psi(s)]^2 \mathrm{e}^{sx} K(x) \mathrm{d}x}{\int \mathrm{e}^{sx} K(x) \mathrm{d}x} > 0 .$$

In particular, the function $s^2 c'(s)$ is increasing so that $2sc' + s^2 c'' > 0$. Hence, at every critical point of c (i.e., $c' = 0$), we have $c'' > 0$. Therefore, there cannot be a local maximum. If there were two local minima, then there would have to be a local maximum in between, which is impossible. □

The slowest speed at which an exponential profile in the linear equation can travel is

$$\hat{c} = \min_{s>0} \frac{1}{s} \ln(RM(s)) . \tag{5.17}$$

We call this speed the *minimal speed of a traveling front in the linear equation*.

The value of $\hat{c}$ can be computed explicitly for the Gaussian kernel. The moment-generating function of the Gaussian kernel (2.25) is

$$M(s) = \exp\left(\frac{\sigma^2 s^2}{2}\right) . \tag{5.18}$$

The dispersion relation and its derivative are

$$c(s) = \frac{\ln(R)}{s} + \frac{\sigma^2 s}{2} \quad \text{and} \quad c'(s) = -\frac{\ln(R)}{s^2} + \frac{\sigma^2}{2} . \tag{5.19}$$

The curve $c(s)$ is strictly convex for $s > 0$. Its unique minimum occurs at the critical value $s^* = \pm\sqrt{\ln(R)/\sigma^2}$ and is given by

$$\hat{c} = c(s^*) = \sqrt{2\sigma^2 \ln(R)} . \tag{5.20}$$

Hence, the minimal speed for the Gaussian kernel is the same as the asymptotic speed c_G that we obtained from the point-release approach in (5.7). Since the Cauchy kernel from the previous section does not have a finite moment-generating function, it does not produce traveling profiles with constant speed.

Many other dispersal kernels have a finite moment-generating function, at least for s in some interval around zero. While the formula in (5.17) gives the minimal traveling-wave speed for those kernels, the minimization usually has to be carried out numerically. Rather than straightforward minimization, Kot et al. (1996) propose the following parametric approach to (5.15). We consider the left and right sides of equation (5.15) as curves in the (c, R)-plane, parameterized by s, and we ask when they intersect. Both curves are nondecreasing and concave up. When $c = 0$, there is no intersection since the left-hand side is the constant one, whereas on the right-hand side, we have $R > 1$ and $M(s) \geq 1$ for a symmetric kernel. As we increase c, the expression on the left-hand side increases, whereas the right-hand side remains the same. For large enough values of c, the curves will intersect. If the moment-generating function grows faster than exponentially for large s, we expect the intersection point to appear at some finite value of s. The moment-generating function of the Gaussian kernel certainly satisfies this condition. At the smallest value of c for which the curves intersect, the two curves will then be tangent, i.e., in addition to (5.15), the derivatives of both sides with respect to s are also equal. Hence, at the minimal traveling-wave speed, $\hat{c}$, the following two equations have to be satisfied simultaneously:

$$e^{s\hat{c}} = RM(s)\,, \qquad \hat{c}e^{s\hat{c}} = RM'(s)\,. \tag{5.21}$$

Dividing the second equation by the first and back-substituting gives us the parametric representation of the slowest speed as

$$\hat{c} = \frac{M'(s)}{M(s)}\,, \qquad R = \frac{e^{sM'(s)/M(s)}}{M(s)}\,. \tag{5.22}$$

With this representation, it is straightforward to plot $\hat{c}$ as a function of R for a given (exponentially bounded) dispersal kernel; see Fig. 5.4 below.

For the Gaussian kernel, (5.22) provides an easier way to calculate $\hat{c}$. Substituting M from (5.18), we find

$$\hat{c} = \sigma^2 s\,, \qquad R = e^{\sigma^2 s^2/2}\,. \tag{5.23}$$

Solving the second equation for s and inserting into the first results in the expression in (5.20).

For the Laplace kernel, the parametric approach leads to an explicit formula for the minimal traveling-wave speed. The moment-generating function of the Laplace kernel (2.27) with dispersal parameter a is given by

$$M(s) = \frac{a^2}{a^2 - s^2}\,, \qquad |s| < a\,. \tag{5.24}$$

The parametric representation in (5.22) becomes

$$\hat{c} = \frac{2s}{a^2 - s^2}\,, \quad R = \left(1 - \frac{s^2}{a^2}\right)\exp\left(\frac{2s^2}{a^2 - s^2}\right)\,. \tag{5.25}$$

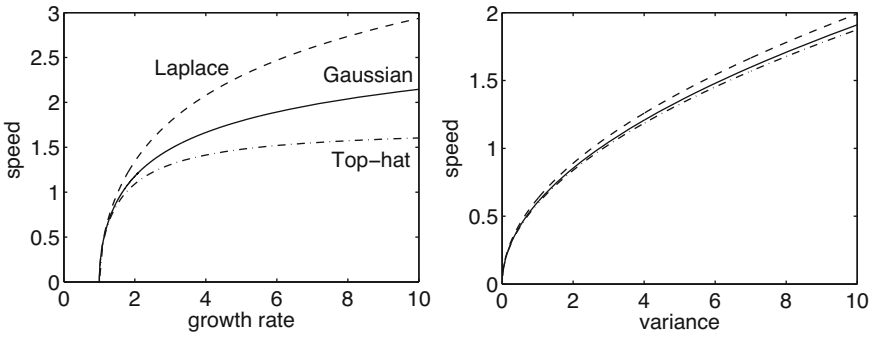

Fig. 5.4 Relationship between minimal traveling-wave speed $\hat{c}$ and growth rate R (left plot), respectively, variance σ^2 (right plot), for three different dispersal kernels: Gaussian (solid), Laplace (dashed), and top-hat (dash-dot). In the right plot, we fixed $\sigma^2 = 1$; in the left plot $R = 1.2$.

We can use this representation in two ways. One is to simplify by setting $\tilde{s} = \frac{2s^2}{a^2 - s^2}$ or $s^2 = \frac{a^2\tilde{s}}{2+\tilde{s}}$ to obtain

$$R = \frac{2\mathrm{e}^{\tilde{s}}}{2+\tilde{s}} \quad \text{and} \quad a\hat{c} = \frac{2sa}{a^2 - s^2} = \frac{\tilde{s}a}{s} = \sqrt{\tilde{s}^2 + 2\tilde{s}}\,. \tag{5.26}$$

The expression for R is now independent of a and is an increasing function of $\tilde{s}$. Hence, for each $\tilde{s}$ there is a unique R (numerically easy to find) that we can substitute into the equation for $\hat{c}$ to find the speed.

Another approach is to rewrite the equation for R in (5.25) as

$$\frac{R\mathrm{e}^2}{2}\frac{2a^2}{a^2 - s^2} = \exp\left(\frac{2a^2}{a^2 - s^2}\right)\,. \tag{5.27}$$

This equation can be solved using the -1-branch of the Lambert W function to obtain s and subsequently $\hat{c}$ as

$$\hat{c} = -\frac{1}{a}W_{-1}\left(\frac{-2}{R\mathrm{e}^2}\right)\sqrt{\frac{2}{W_{-1}\left(\frac{-2}{R\mathrm{e}^2}\right)} + 1}\,. \tag{5.28}$$

Details can be found in Bourgeois (2016).

In Fig. 5.4, we illustrate how the minimal traveling-wave speeds for the Gaussian, the Laplace, and the top-hat kernel (see Table 3.1) depend on the two model parameters: the growth rate and the variance of the kernel. The speed is increasing in both parameters. The speed for the Gaussian kernel is slower than for the Laplace kernel but faster than for the top-hat kernel. When the variance is fixed, the speed for the top-hat kernel is bounded by its finite support: since no individual can move farther than $\beta = \sqrt{3\sigma^2}$, the distance moved per generation, $\hat{c}$, cannot exceed that number. In the left plot, we have $\sigma^2 = 1$, so that the minimal traveling-wave speed is bounded by $\sqrt{3} \approx 1.732$. When the growth rate is fixed, the curves for all three kernels are very close together (right plot). The curves for $\hat{c}$ as a function of R may intersect for different kernels; see Fig. 4 in Kot et al. (1996). This phenomenon can arise if one of the kernels is highly concentrated near zero but has bounded support, e.g., $K(x) = a - b\ln|x|$.

Figure 1 in Lutscher (2007) shows that the curves for $\hat{c}$ as a function of σ^2 are similar for several other kernels. In other words, the speed for the Gaussian kernel seems to approximate the speed for other kernels with the same growth rate and variance reasonably well. We will discuss this question further in Chap. 10 in the context of approximations.

5.4 Nonlinear Growth Functions

When we use a more realistic, nonlinear growth function, an explicit solution such as (5.3) for the linear model with point release is no longer available. Which of the results and insights from the linear theory still hold in the nonlinear case? It turns out that all the results that can carry over do so as long as there is no Allee effect (which we assume throughout this chapter). To begin, we consider a special class of growth functions. We shall assume that the extinction state is unstable and that there is a positive, globally stable steady state (which we can and shall assume to be unity). We shall also assume that the growth function is monotone. These assumptions are expressed as follows:

(F1) $F(0) = 0$ and $F(1) = 1$ are the only two fixed points of F.
(F2) Fixed point $N = 0$ is unstable and $N = 1$ is stable.
(F3) F is continuous and nondecreasing.
(F4) F is differentiable at zero with $F'(0) > 1$ and linearly bounded, i.e., $F(N) \leq F'(0)N$.

We shall relax the monotonicity assumption in (F3) later in the chapter. We recall that throughout the chapter, we assume that dispersal is unbiased, i.e., $K(x) = K(-x)$.

For the nonlinear IDE, a traveling front satisfies not only a shift condition similar to that in (5.14) but also asymptotic conditions. Specifically, the limits at $\pm\infty$ need to correspond to fixed points of growth function F. Hence, a traveling wave to the right with speed $c > 0$ of IDE (5.1) is a function $N^*(x)$ that satisfies the equation

$$N^*(x - c) = Q[N^*](x) = \int_{-\infty}^{\infty} K(x - y)F(N^*(y))\mathrm{d}y \,, \tag{5.29}$$

with asymptotic conditions $\lim_{x\to\infty} N^*(x) = 0$ and $\lim_{x\to-\infty} N^*(x) = 1$. By symmetry, if there is a rightward traveling-front solution with speed c and asymptotic conditions as stated, then there is also a leftward traveling-front solution with speed $-c$ and asymptotic conditions interchanged. Under conditions (F1)–(F4), we can get a bound for the speed of a traveling front in the nonlinear equation from the minimal speed in the linear equation.

Lemma 5.2 *Assume that the moment-generating function of K exists in some neighborhood of zero and that the growth function satisfies $F(N) \leq F'(0)N$. Then the minimum traveling-front speed of the nonlinear equation (5.29) is bounded above by $\hat{c}$ in (5.17), where $R = F'(0)$.*

Proof We assume that a traveling front exists and denote it by N^*. Since F has no Allee effect, we have the inequality

$$N^*(x - c) = \int_{-\infty}^{\infty} K(x - y)F(N^*(y))\mathrm{d}y \leq F'(0) \int_{-\infty}^{\infty} K(x - y)N^*(y)\mathrm{d}y \,. \tag{5.30}$$

Taking an exponential transform on both sides leads to the bound $e^{sc} \leq F'(0)M(s)$. Therefore, the minimum c is bounded by $\hat{c}$. □

It is much harder to show, but true, that the minimal speeds in the linear and nonlinear case are equal and that traveling fronts for the nonlinear case exist under certain assumptions on F and K. To proceed in this direction, we introduce a new measure of the speed of spread, the *asymptotic spreading speed*. This concept is independent of the assumption that a traveling front exists and requires no special initial condition as in the point-release scenario. Yet, it will turn out to be closely related to both of these.

The Asymptotic Spreading Speed

The notion of an *asymptotic spreading speed* (Aronson and Weinberger 1975) can be motivated as follows. Suppose a population is newly introduced into a confined region. This population is said to spread with asymptotic speed c^* if an observer who travels at some speed $c > c^*$ will eventually be ahead of the population whereas an observer who travels at speed $c < c^*$ will eventually be surrounded by the population. Mathematically, these considerations can be expressed as follows.

Definition 5.1 The number c^* is called the *asymptotic spreading speed* if it satisfies the conditions

$$\limsup_{t\to\infty} \max_{|x|>(c^*+\epsilon)t} N_t(x) = 0\,, \quad \liminf_{t\to\infty} \min_{|x|<(c^*-\epsilon)t} N_t(x) \geq \beta > 0 \tag{5.31}$$

for any small $\epsilon > 0$ and some $\beta > 0$, where $N_0 \not\equiv 0$ is compactly supported and N_t is defined by the iteration in (5.29).

A priori, it is not clear that such an asymptotic spreading speed exists. Naturally, some conditions on the dispersal kernel and growth function are necessary. For example, for the linear growth function and the Cauchy kernel, no asymptotic spreading speed exists; see Sect. 5.2. In the following, we discuss the most relevant results about the existence of an asymptotic spreading speed according to the properties of the growth function F, always assuming that the dispersal kernel is exponentially bounded.

Spread with Compensatory Growth

Weinberger (1982) proves the existence of a spreading speed and several of its properties for the general recursion operator

$$N_{t+1} = Q[N_t]\,, \tag{5.32}$$

defined on a space of continuous functions on $\mathbb{R}$. In particular, the theorem below applies not only to IDEs but also to other dynamic equations, e.g., to the time-1-map of an appropriate reaction–diffusion equation.

To state the assumptions and results, we will frequently identify a number with a constant function. For two continuous functions, $N, \tilde{N}$, we write $N \geq \tilde{N}$ if $N(x) \geq \tilde{N}(x)$ for all x. We denote by $\mathscr{C}_{[0,1]}$ the space of continuous functions on $\mathbb{R}$ with values in the interval [0, 1]. The following theorem summarizes results from Theorems 6.5 and 6.6 by Weinberger (1982).

Theorem 5.1 *Consider the following properties of operator Q on the space $\mathscr{C}_{[0,1]}$ of continuous functions.*

(i) Translation invariance: $Q[N(\cdot - a)](x) = Q[N](x - a)$ for all $a \in \mathbb{R}$.
(ii) Invariance of $\mathscr{C}_{[0,1]}$: $N \in \mathscr{C}_{[0,1]} \Rightarrow Q[N] \in \mathscr{C}_{[0,1]}$.
(iii) Fixed points: $Q[0] = 0$, $Q[1] = 1$, $Q[a] > a$ for $a \in (0, 1)$.
(iv) Monotonicity: $0 \leq N \leq \tilde{N} \leq 1 \Rightarrow Q[N] \leq Q[\tilde{N}]$.
(v) Continuity: If $\{f_j\} \subset \mathscr{C}_{[0,1]}$ and $f_j \to f$ uniformly on compact subsets of $\mathbb{R}$, then $Q[f_j] \to Q[f]$ pointwise as $j \to \infty$.
(vi) Compactness: Every sequence $\{f_j\}$ in $\mathscr{C}_{[0,1]}$ has a subsequence $\{f_{j_i}\}$ such that $\{Q[f_{j_i}]\}$ converges uniformly on every bounded subset of $\mathbb{R}$.

Assume that Q in (5.32) satisfies (i)–(v). Then there exists an asymptotic spreading speed $c^* > 0$ for Q. If, in addition, (vi) holds, then for every $c \geq c^*$ there exists a continuous traveling-wave solution $N_t(x) = W(x - ct)$ of Q with $W(\infty) = 0$ and $W(-\infty) = 1$. No such traveling wave exists for $c < c^*$.

For the purpose of this theorem, the definition of the asymptotic spreading speed can be strengthened in that the second condition in (5.31) can be replaced by

$$\lim_{t\to\infty} \min_{|x|<(c^*-\epsilon)t} N_t(x) = \lim_{t\to\infty} \max_{x\in\mathbb{R}} N_t(x) = 1 \,, \tag{5.33}$$

provided the initial condition is bounded between zero and one. Hence, the density converges to the positive steady state behind the front.

As stated, the preceding theorem does not give a way to calculate the spreading speed. Weinberger (1982) gives a general construction to define c^* and uses it in the proof of the theorem. We present this construction in Chap. 13.8. Weinberger (1982) uses super- and sub-solutions to prove that the asymptotic spreading speed is given by the linearized formula from (5.17) if certain additional conditions are satisfied. We include this statement in the next theorem, where we apply the previous theorem to IDEs and relate the properties of the growth function F to those of operator Q.

Theorem 5.2 *Consider operator Q from (5.29). Assume that K is continuous and that its moment-generating function exists for all $s \in \mathbb{R}$. Assume that the growth function satisfies conditions (F1)–(F4). Then there exists an asymptotic spreading speed, c^*, for Q. Furthermore, c^* equals the minimal traveling-wave speed $\hat{c}$ from (5.17), where $R = F'(0)$. Finally, for all $c \geq c^*$ there exists a monotone traveling-*

front solution of (5.29), connecting zero and one with speed c, but for $c < c^*$ no such traveling-front solution exists.

Proof We will show that the assumptions on F and K guarantee that conditions (i)–(vi) in Theorem 5.1 are satisfied for Q from (5.29). We discuss the claim $\hat{c} = c^*$ separately below.

Translation invariance follows from the properties of the convolution operator by a change of variables. Since F is monotone increasing and has zero and one as fixed points, the interval $[0, 1]$ is invariant for the map F. Since K is nonnegative and integrates to unity, Q maps functions bounded between zero and one into functions with the same bounds.

Since K integrates to unity, constant functions are mapped to constant functions under Q. Since F has zero and one as fixed points, the constant functions zero and one are fixed points for Q. Since $F'(0) > 1$ and since zero and one are the only fixed points of F in $[0, 1]$, we must have $F(a) > a$ for all $0 < a < 1$. Hence, the same is true for constant functions under Q. Monotonicity of Q follows from monotonicity of F since K is nonnegative.

We prove continuity of Q under the slightly stronger assumption that F is Lipschitz. We denote by L the Lipschitz constant of F. Consider a sequence of functions $\{f_j\}$ in $\mathscr{C}_{[0,1]}$ that converges uniformly on compact subsets to f. Then for every $m > 0$ we have the estimate

$$\begin{aligned}
|Q[f_j](x) - Q[f](x)| &= \left| \int K(x-y)(F(f_j(y)) - F(f(y)))\mathrm{d}y \right| \\
&\le \left| \int_{|y|>m} K(x-y)(F(f_j(y)) - F(f(y)))\mathrm{d}y \right| \\
&\quad + \left| \int_{|y|\le m} K(x-y)(F(f_j(y)) - F(f(y)))\mathrm{d}y \right| \\
&\le 2\int_{|y|>m} K(x-y)\mathrm{d}y + L\int_{|y|\le m} K(x-y)|f_j(y) - f(y)|\mathrm{d}y\,.
\end{aligned}$$

Since the kernel integrates to unity, we can choose m large to make the first term arbitrarily small. Since f_j converges uniformly on compact subsets, we can choose j large (for fixed m) to make the second term arbitrarily small. Hence, $Q[f_j] \to Q[f]$ pointwise.

To prove that Q is compact is a little more involved but uses some of the same ideas (see, e.g., Bourgeois 2016). We choose a sequence $\{f_j\}$ in $\mathscr{C}_{[0,1]}$, a compact interval I, and some $m > 0$. Then we define the sequence

$$\tilde{f}_j(x) = \int_{-m}^{m} K(x-y)F(f_j(y))\mathrm{d}y\,, \qquad x \in I\,.$$

Boundedness of F gives us uniform boundedness of $\tilde{f}_j$. Since K is continuous, it is uniformly continuous on compact sets. Therefore, $\tilde{f}_j$ are equicontinuous. By the Arzelà–Ascoli theorem, there is a convergent subsequence $\tilde{f}_{j_i} \to f$. The same splitting of the integral as in the proof of continuity above then gives us uniform convergence of $Q[f_t]$ on bounded subsets of $\mathbb{R}$. □

We have not yet proved the claim $c^* = \hat{c}$. To show that the spreading speed must be bounded above by the speed of the linear equation with $R = F'(0)$ is fairly straightforward, but the reverse inequality is much harder; we refer to Weinberger (1982). Both proofs rely on monotonicity, but the latter requires the careful construction of a sub-solution (compare the proof of Lemma 4.2).

Lemma 5.3 *Under the assumptions of the previous theorem, we have* $c^* \leq \hat{c}$.

Proof If N_0 is compactly supported with $0 \leq N_0(x) \leq 1$ for all $x \in \mathbb{R}$, then for each $s > 0$ one can find a constant A such that $N_0(x) < A\exp(-sx)$ for all $x \in \mathbb{R}$. The solution of the nonlinear equation is bounded by the solution of the linear equation because of assumption (F4):

$$\int K(x, y)F(N_t(y))\mathrm{d}y \leq F'(0)\int K(x, y)N_t(y)\mathrm{d}y\ . \tag{5.34}$$

Hence, the solution N_t of the nonlinear equation with initial condition N_0 cannot spread faster than the solution of the linear equation with initial condition $A\exp(-sx)$. Choosing the value of s that corresponds to $\hat{c}$ gives the stated inequality. □

The result that the spreading speed of the nonlinear equation is equal to the spreading speed of the linearized (at zero) equation (which, in turn, is equal to the minimal traveling wave speed of the linearized equation) is known as *linear determinacy* (Lewis et al. 2002). The *linear conjecture* is the belief that a system is linearly determinate under certain conditions (van den Bosch et al. 1990). One of these conditions is the linear boundedness condition on the growth function, which excludes an Allee effect. We consider an Allee effect in Chap. 6.

Spread with Overcompensatory Growth

The Ricker function in (2.19) with parameter $0 < r < 1$ is monotone and satisfies conditions (F1)–(F4). However, with $1 < r < 2$, it is not monotone on the interval $[0, 1]$; see Fig. 5.5. Conditions (F1), (F2), and (F4) above are satisfied, but the second part of (F3) is not. In Chap. 2, we saw that solutions of the nonspatial model approach the stable state $N = 1$ with decaying oscillations. A similar pattern can occur for the logistic growth function in (2.20).

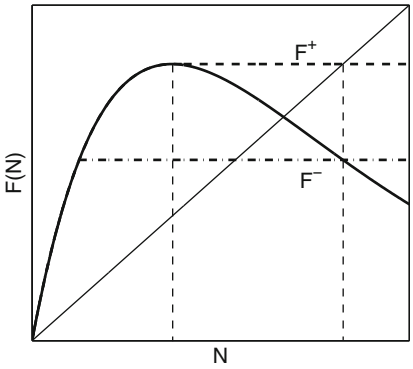

Fig. 5.5 Illustration of the definition of $F^{\pm}$. The solid curve is the Ricker growth function. The increasing portion of the Ricker function together with the dashed horizontal line is the function F^{+}. The dash-dot horizontal line together with the increasing beginning of the Ricker function is F^{-}. The thin dashed vertical lines indicate the location of the maximum ($\hat{N}$) and its value ($\hat{F}$).

We cannot expect the existence of a monotone traveling-front profile. Nonetheless, we can use Theorem 5.2 to show the existence of a spreading speed even with nonmonotone dynamics. The fundamental idea goes back to work by Thieme (1979) on integral equations in continuous time. Several authors apply this idea to IDEs with nonmonotone growth functions (Hsu and Zhao 2008; Li et al. 2009; Yu and Yuan 2012; Yi and Zou 2015). We present some of their ideas and results here.

We shall assume that the growth function satisfies (F1)–(F4) except the monotonicity assumption in (F3). Instead, we assume that there exists some $\hat{N} \in (0, 1)$ such that F is increasing for $0 \le N < \hat{N}$ and decreasing for $N > \hat{N}$. Furthermore, we assume that $|F'(1)| < 1$ so that the unique fixed point is stable. We define functions $F^{\pm}$ as follows (see Fig. 5.5): We set $\hat{F} = \max\{F(N)|0 \le N \le 1\} = F(\hat{N})$ and define

$$F^{+}(N) = \max_{\tilde{N} \le N}\{F(\tilde{N})\}\,, \qquad F^{-}(N) = \min\{F(N), F(\hat{F})\}\,. \tag{5.35}$$

Finally, we define $Q^{\pm}$ as in (5.29) with F replaced by $F^{\pm}$, respectively.

With this construction, we can bound solutions of $N_{t+1} = Q[N_t]$ from above and below by solutions of $N_{t+1} = Q^{\pm}[N_t]$, respectively.

Theorem 5.3 *Under the assumptions and definitions in the previous paragraph, the following hold.*

1. *$F^{\pm}$ satisfy conditions (F1)–(F4).*
2. *$Q^{\pm}$ satisfy the assumptions of Theorem 5.2; in particular, their respective spreading speeds $c^{*}_{\pm}$ exist.*
3. *Q has a spreading speed c^{*}, and $c^{*}_{-} = c^{*} = c^{*}_{+}$.*

Proof We sketch the main geometric idea of the proof but refer to Hsu and Zhao (2008), Li et al. (2009), and Yi and Zou (2015) for technical details. The construction in Fig. 5.5 guarantees that $F^{\pm}$ satisfy the conditions of Theorem 5.2, which implies that the respective spreading speeds, $c^*_{\pm}$, of operators $Q^{\pm}$ exist and are determined by the respective linearizations at zero. The construction also shows that $F^+(N) = F^-(N)$ for small enough N. The latter property implies that $(F^+)'(0) = (F^-)'(0)$ so that $c^*_- = c^*_+$.

Next, we note that $F^-(N) \le F(N) \le F^+(N)$, which implies that the same inequalities hold for the corresponding operators, i.e., $Q^-[N] \le Q[N] \le Q^+[N]$. Hence, for a given initial condition, the solution with operator Q is sandwiched between the solutions with Q^- and Q^+. Since the latter two spread at the same speed, the former has to spread at that speed as well. □

Theorem 5.2 also guarantees the existence of monotone traveling waves that connect the zero state with the positive state for $Q^{\pm}$. The situation for Q is a bit more delicate. As previously discussed, one cannot expect a traveling wave, if it exists, to be monotone. The plots in Fig. 5.6 illustrate monotone (left) and nonmonotone (right) traveling fronts with the Ricker function for different parameter values with a characteristic function[2] as initial condition. In both cases, the profile converges to zero ahead of the front and to the positive fixed point behind the front. A general proof of this property and whether it holds for all $c \ge c^*$ turns out to be surprisingly difficult. The respective works by Hsu and Zhao (2008), Li et al. (2009), and Yu and Yuan (2012), Yi and Zou (2015) each use slightly different conditions; see also

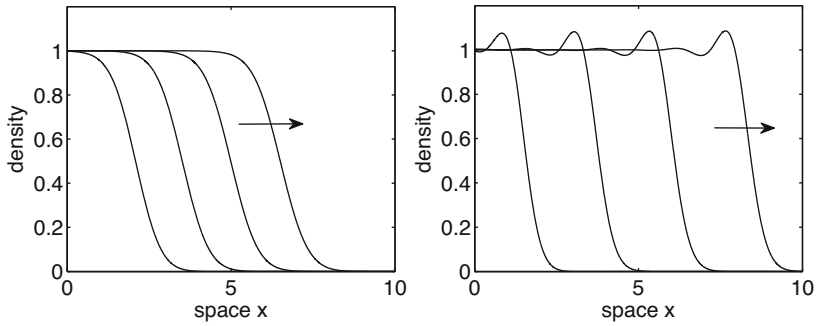

Fig. 5.6 Illustration of monotone and nonmonotone traveling fronts in the IDE with Ricker growth function and Gaussian dispersal kernel. Parameters are $\sigma^2 = 0.1$, $r = 0.8$ (left), and $r = 1.8$ (right). The initial condition is the characteristic function on $(-\infty, 0)$; the profile is plotted every four time steps.

[2]The *characteristic function* or indicator function of a set takes the value one on the set and zero everywhere else. It is often denoted by χ. We will frequently use the characteristic function of a half line as initial conditions in numerical simulations of traveling fronts. For example, $\chi_{(-\infty,0]}(x) = 1$ if $x \le 0$ and $\chi_{(-\infty,0]}(x) = 0$ if $x > 0$.

Lin (2015). The conditions in Yi and Zou (2015) are particularly simple to verify geometrically. Their Theorem 4.1 implies the following result.

Theorem 5.4 *Assume that (F1), (F2), and (F4) hold. Assume further that* $N = 1$ *is the only fixed point of* F^2. *Then for all* $c \geq c^*$, *there exists a traveling wave,* $N^*(x - c) = Q[N](x)$, *with* $N^*(\infty) = 0$ *and* $N^*(-\infty) = 1$.

When the positive fixed point of the growth function is unstable, one cannot expect a traveling wave to converge to that point. For example, the positive fixed point of the Ricker function becomes unstable through a flip bifurcation, and a stable two-cycle emerges. Accordingly, solutions in the spatial model may show oscillations in the wake of an invasion front (Bourgeois 2016). We discuss and illustrate these phenomena in Chap. 11.

5.5 Further Reading

Spreading phenomena and traveling waves were studied in reaction–diffusion equations, starting with Fisher (1937), long before they were studied in IDEs, e.g., Weinberger (1978) and references therein. Spreading phenomena in continuous-time integral models are reviewed in Metz et al. (1999). A survey that includes continuous and discrete-time equations can be found in Zhao (2009).

The notion of the asymptotic spreading speed was also originally introduced for reaction–diffusion equations (Aronson and Weinberger 1975). It was, however, studied via the time-1-map, so that the continuous-time equation was transformed to a discrete-time recursion, similar to an IDE. Subsequent work focused on discrete-time equations and was motivated mostly by population genetics (Weinberger 1978, 1982). The traveling-front profile is unique and solutions with monotone initial data converge to this traveling front (Lui 1982a). Solutions with compactly supported initial data converge to a double traveling-front profile when (F1)–(F4) hold (Lui 1982b).

Weinberger (1982) originally restricts the dispersal range of any individual to some finite limit, which would require a compactly supported dispersal kernel. Weinberger's proof, however, when applied to IDEs, only requires that the moment-generating function of the dispersal kernel exist on the whole real line. Extensions by Hsu and Zhao (2008) and Weinberger and Zhao (2010) show that the formulas hold if the moment-generating function is finite at a single nonzero value. They also show that the asymptotic spreading speed is infinite if the moment-generating function is infinite for all nonzero values, thereby clarifying the behavior of spread with heavy-tailed kernels. Continuity of the dispersal kernel is also not necessary for these results to hold. It is usually sufficient to require that K be Lebesgue integrable to prove the existence of traveling fronts (Hsu and Zhao 2008; Yu and Yuan 2012).

The theory of spreading speeds and traveling fronts can be formulated in any finite space dimension. One then defines a spreading speed for any given direction (unit vector) and planar traveling waves moving in that direction. The results by

Weinberger (1982) and subsequent works hold in that generality. The stability of monotone traveling wave fronts with a Gaussian dispersal kernel was investigated in two dimensions by Lin et al. (2010) and in any finite dimension by Miller and Zeng (2013).

Throughout this chapter, we assumed that dispersal is unbiased so that the dispersal kernel is symmetric. Many results in this chapter carry over to asymmetric dispersal if the direction of spread is properly accounted for (Yi and Zou 2015), but some caution is necessary. We discuss biased dispersal in detail in Sect. 12.2.

The spreading speed is only an asymptotic quantity that we expect to observe for large times. It is nonetheless a useful quantity for applications since it turns out that "large" is not very large at all. In simulations, we see that a solution develops into a traveling wave with speed close to the asymptotic spreading speed after very few generations (e.g., less than 10 generations in Fig. 5.3). Accordingly, Watkinson et al. (2000) use the speed formula for the linear model to estimate the expected spatial extent of a locally introduced annual grass (*Vulpia ciliata*) within a time frame of 20 years. More examples can be found in Kot (2003) and Lewis et al. (2016).

The Gaussian and the Cauchy kernels represent two extremes: the tails of the former are exponentially bounded (thin tailed), whereas the tails of the latter decay like a power law (fat-tailed). Accordingly, the moment-generating function of the former is well defined, whereas the latter has no finite moments of any order. More generally, kernels whose tails decay slower than exponentially are called heavy tailed. While their moment-generating function does not exist, their moments

$$\int_{-\infty}^{\infty} x^n K(x)\mathrm{d}x\,, \qquad n = 1, 2, 3, \ldots\,, \tag{5.36}$$

may still be finite. One example of such a kernel is the exponential square root kernel

$$K(x) = \frac{a^2}{4} \exp\left(-a\sqrt{|x|}\right)\,. \tag{5.37}$$

For these heavy-tailed kernels, the population density in generation t is asymptotically distributed as (Kot et al. 1996)

$$N_t(x) \sim R^t K(x)\,, \qquad |x|, t \to \infty\,. \tag{5.38}$$

From this explicit formula, we calculate the spatial extent of the population with the exponential square root kernel at time t to be

$$x_t = \frac{1}{a^2}\left[t \ln R + \ln\left(\frac{a^2}{4\tilde{N}}\right)\right]^2. \tag{5.39}$$

Hence, the spatial extent grows quadratically in time, and therefore the speed of spatial spread grows linearly in time. Liu and Kot (2019) present a much more

detailed analysis of how invasions accelerate as a function of heavy-tailed dispersal kernels, using the theory of regular variation.

The versatility with which IDEs incorporate non-Gaussian dispersal patterns, and the phenomenon of accelerating invasions for heavy-tailed kernels has attracted a lot of attention among ecologists. The sensitive dependence of spread rates on the tails of a dispersal kernel, however, poses significant challenges for empiricists. Since it is difficult, if not impossible, to track individuals that disperse very far, it is extremely challenging to decide the decay rate of an empirical dispersal kernel. Pielaat et al. (2006) propose a sampling design for seed traps, optimized to estimate invasion speeds for IDEs, i.e., for catching the density in the tails of the kernel. Nathan et al. (2003) review methods for long-distance dispersal estimates. Bianchi et al. (2009) point to the importance of selecting an appropriate kernel in the context of colonization times, i.e., when calculating the time that it takes for a certain number of individuals to arrive at one site from another.

Formula (5.17) for the minimal speed of traveling fronts in the linear equation does not actually use the dispersal kernel but rather its moment-generating function. Consequently, Clark et al. (2001b) derive an estimator for spread rates from data using the empirical moment-generating function, thereby circumventing the difficulty of having to estimate the decay rate of the tails. This idea was later expanded by Lewis et al. (2006), who also discuss differences between one- and two-dimensional estimates.

In reality on a bounded planet, of course, no dispersal kernel has truly heavy or even infinite tails. Similarly, no invasion can continue forever, so that the asymptotic speed can never be observed. Clark et al. (2001a) consider discrete individuals and track the location of the farthest-forward individual. They obtain a finite speed of spread even when dispersal distances are drawn from heavy-tailed kernels. Following up, Clark et al. (2003) explore the influence of uncertainty and estimate speeds for potentially heavy-tailed kernels. Demographic stochasticity may also lead to bounded spread rates even for kernels that produce accelerating waves for the deterministic mean-field model (Jacobs and Sluckin 2015).